Filtering point spread function in backprojection cone beam CT and its applications in long object imaging

K.C. Tam[a], G. Lauritsch[b], and K. Sourbelle[c]
[a]Siemens Corporate Research, Inc. Princeton, NJ 08540
[b]Siemens AG, Medical Solutions, Erlangen, Germany
[c]Institute of Medical Physics, University of Erlangen, Erlangen, Germany

Abstract

In backprojection cone beam CT each cone beam image is first filtered, then 3D backprojected into the object space. In this paper the filtering point spread function (PSF) is derived analytically. It is found that the PSF is in the form of 1D Hilbert transforms. The PSF finds applications in a number of aspects in long object imaging, including backprojection implementation of the local ROI algorithm, elimination of the second intersection artifact, reduced pitch spiral scanning for increased S/N, and reduction of spiral overscan in long object imaging.

I. Filtering point spread function

Backprojection cone beam image reconstruction [1,2,8,9] consists of two steps: a 2D step and a 3D step. First, each cone beam image undergoes 2D filtering. Then the filtered image is backprojected into the object space in the 3D step. 2D filtering consists of the following 4 sub-steps: (1) 1D projection of the cone beam image at angle θ; (2) Differentiation of the projections; (3) Backprojection of the projection derivative in the same direction. Sub-steps (1) through (3) are carried out for θ in the angular range [η-π/2, η+π/2] forming a backprojection image, where η is the angular displacement (from the *u* axis) of the direction $\vec{t}$ which is the projection of the scan path tangent on the detector. Finally, (4) take the derivative of the backprojection image in the projected scan path direction $\vec{t}$. The filtered image Y after these 4 sub-steps can be written as:

$$Y = D_t\{\int d\theta[B(\theta)D_{r(\theta)}(\theta)P(\theta)]\}M(X) \qquad (1)$$

where X is the cone beam image, M the data-combination masking operation [5], P(θ) the projection operation in the direction θ, $D_r(\theta)$ the differentiation operation w.r.t. the spatial variable *r* for the projection at angle θ, B(θ) the backprojection operation in the direction θ, and D_t the differentiation (spatial) operation in the projected scan path direction $\vec{t}$. The reason that the projection and backprojection operations in Equation (1) are carried out for θ in the angular range [η-π/2, η+π/2] is to ensure that the product of the derivative d/dt with d/dr has the same sign for all the angles within the range; otherwise the signs of the product at different angles will be inconsistent.

The sub-steps (1) through (3) can be combined into a 1D convolution step as follows:

Theorem 1. The combined operations of sub-steps (1) through (3) in the angular range [χ-π/2, χ+π/2] is equivalent to the 1D Hilbert transform in the direction of the unit vector $\vec{\chi}$ which makes an angle χ with the detector *u* axis:

$$H_{\vec{\chi}} = \int_{\chi-\pi/2}^{\chi+\pi/2} d\theta\, B(\theta) D_{\vec{r}(\theta)} P(\theta)\,, \qquad (2)$$

where $H_{\vec{\chi}}$ is the 1-D Hilbert transform in the direction of the unit vector $\vec{\chi}$. $H_{\vec{\chi}}$ can be expressed as a 2-D function in Fourier space

$$H_{\vec{\chi}}(\vec{k}) = i \cdot \mathrm{sign}(\vec{\chi}\cdot\vec{k})\,. \qquad (3)$$

For the cases where the projection/backprojection angular range is less than π, we have the following results:

Theorem 2. The combined operations of sub-steps (1) through (3) in the angular range [θ_1, θ_2], where $\theta_1 \in$ [η-π/2, η+π/2] and $\theta_2 \in$ [η-π/2, η+π/2], is equivalent to the sum of two 1D Hilbert transforms:

$$\int_{\theta_1}^{\theta_2} d\theta\, B(\theta) D_{\vec{r}(\theta)} P(\theta) = 1/2\left(H_{\overline{(\theta_2-\pi/2)}} + H_{\overline{(\theta_1+\pi/2)}}\right) \qquad (4)$$

II Backprojection implementation of local ROI algorithm

An exact backprojection driven spiral scan cone beam CT algorithm for ROI reconstruction using the local ROI technique was reported in [3,4]. For views in the interior of the spiral where the entire cone beam images undergo the filtering operation in Equation (1), the 2D filtering operation can be simplified to the efficient 1D ramp filtering operation in the direction $\vec{t}$. For the views near the two ends of the spiral, the projection operation P(θ) is applied to only part of the masked cone beam image M(X). This is illustrated in Figure 1 which shows the projection operation for the cone beam images in the view angular range [π, 2π] measured from the spiral top. The point C_0 on the *u* axis is determined by the angular displacement of the current source position from the spiral top. During the projection operation, the line integrals on line segments which cross the *u* axis to the left of C_0 are computed

between the *u* axis and the bottom mask boundary, and the line integrals on line segments which cross the *u* axis to the right of C_0 are computed between the top and the bottom mask boundary.

Applying Equations (2) and (4) yields the result that the $\int d\theta[B(\theta)D_r(\theta)P(\theta)]$ portion of the 2D filtering can be formulated as a superposition of spatially variant 1-D Hilbert transforms $H_{\vec{t}}$, $H_{\vec{u}}$ and $H_{\vec{\rho}(u,v)}$ in the directions $\vec{t}$ of the projection of the tangent of the spiral path, $\vec{u}$ of the horizontal detector axis and $\vec{\rho}(u,v)$ of the unit vector pointing from the point C_0 to the detector pixel (u,v), respectively [10]. These 1-D Hilbert transforms are illustrated in Figure 2.

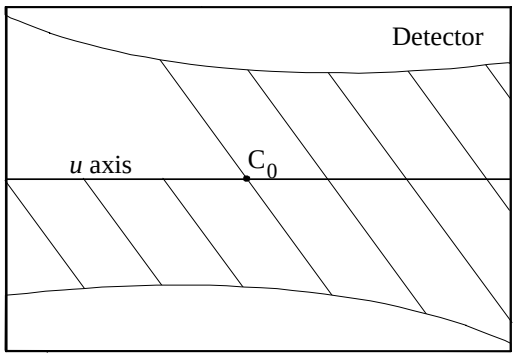

Figure 1. Limits for integration line segments for source positions in the angular range [π,2π] from the spiral top

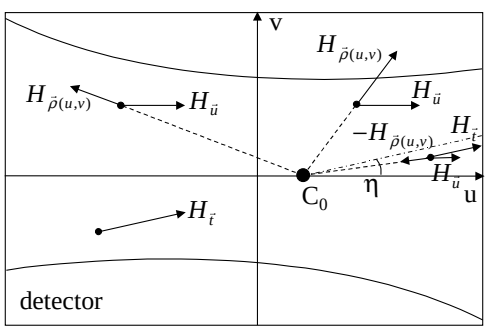

Figure 2: 1-D Hilbert transforms contributing to the filtering of a cone-beam projection around the upper border of the ROI as illustrated in Figure 1

III. Elimination of Second Intersection Artifacts

A key part of the exact spiral cone beam CT reconstruction algorithm is the masking operation M to restrict the projection data to the appropriate angular range required for data combination [5]. The mask consists of a top curve and a bottom curve formed by projecting on the detector the spiral turn above and the turn below from the current source position. Such masking procedure corresponds for the most part to the angular range bound by the prior and the subsequent source positions for data combination. Portions of some line integrals intersecting the mask, however, do not conform to the proper data combination angular range. Consider the top mask boundary and the line L illustrated in Figure 3, where the spiral path which projects onto the mask boundary scans from right to left. Line L intersects the mask boundary at 2 points M_1 and M_2, in other words the integration plane defined by the line L and the current source position intersects the scan path at M_1, M_2, and the current source position. It can be easily seen that M_1 is the next source position after the current one, and M_2 is the next source position after M_1. Thus the portion of the line segment that corresponds to the data combination angular range, i.e. the x-ray data in the angular range bounded by the previous source position below and the next source position above, is the segment to the right of M_1. It is this segment alone that should be included in the projection operation P(θ), i.e. line integration.

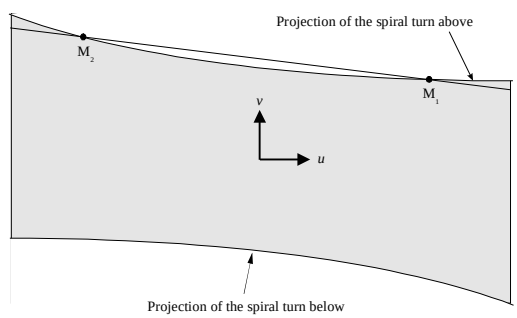

Figure 3. A line of integration intersecting the top mask two times.

In the literature it has been shown [8,9] that the filtering operation of Equation (1) can be simplified using techniques such as 1D ramp filtering, Fourier space convolution, or linogram. In arriving at these results it is assumed that the entire line segment is included in the projection operation. That is to say not only the segment to the right of M_1 but also the segment to the left of M_2 is

included in the projection operation. Such unneeded contribution to projection occurs whenever the line of integration intersects the mask boundary more than once. We refer to such cases as second intersection artifacts.

Errors arising from such line integration occur on the line segment after the second intersection point M_2. A method to correct for these artifacts in backprojection cone beam CT image reconstruction was reported in [6]. It was shown that the projection lines that intersect the top mask boundary more than once are those that lie within the angular range $\mathscr{A}_1 = [\tau(-W/2)-\pi/2, \tau(\infty)+\pi/2]$, where $\tau(\infty)$ is the angle the tangent to the top mask boundary at $u = \infty$ makes with the u axis, $\tau(-W/2)$ is the angle the tangent to the top mask boundary at the left edge $u = -W/2$ of the detector makes with the u axis; $\tau(\infty) = \eta = \tan^{-1}(h/2\pi a)$ is also the angle of the projection of the scan path direction on the detector. For the correction of the second intersection artifacts for the upper mask boundary, the combined operation BD_rP is applied to the cone beam image in the limited angular range $\theta \in \mathscr{A}_1$ on the affected portions of the line segments. Applying Equations (2) and (4) yields the result that the $\int d\theta[B(\theta)D_r(\theta)P(\theta)]$ portion of the 2D filtering results in two Hilbert transforms: ($\frac{1}{2} H_{\vec{t}}$) in the directions $\vec{t}$ of the projection of the tangent of the spiral path, and ($\frac{1}{2} H_{\vec{\alpha}}$) in the direction of the unit vector $\vec{\alpha}$ of the line which makes an angle $\alpha \in \mathscr{A}_1$ with the detector u axis, intersects the pixel to be filtered, and tangential to the mask boundary. These two Hilbert transforms are sketched in Figure 4a and 4b respectively.

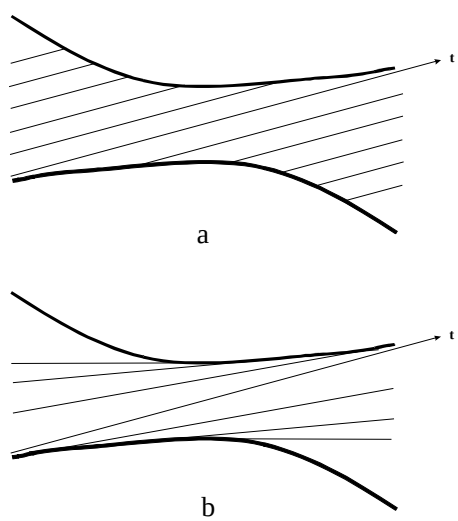

Figure 4. 1D Hilbert transforms: a. $H_{\vec{t}}$ b. $H_{\vec{\alpha}}$

IV. Increasing S/N with reduced pitch scanning

Increase the x-ray dosage in spiral cone beam scan to obtain higher S/N can be achieved by reducing the spiral pitch to 1/3, 1/5, 1/7,…, of the original spiral pitch [11]. Take the case of pitch = 1/3. Instead of combining cone beam data using the standard mask [5], the masked formed by projecting on the detector the second spiral turn above and the second turn below from the current source position is used. Data combination performed in this way contains overlapping portions, and the overlap is such that there is a data redundancy of factor 3. With the reduced pitch = 1/3, the modified mask boundary is the cone beam projection from the current source position of the second spiral turn above and the second spiral turn below, rather than the spiral turn above and the spiral turn below. Since there are approximately 3 times the number of source positions in the pitch = 1/3 scan compared to the pitch = 1 scan, the total radiation exposure in the former is thus increased threefold compared to that of the latter, resulting in higher signal-to-noise ratio.

There is a flaw in this method, however, because a small number of integration planes which intersect the spiral path only once also intersect the spiral path with reduced pitch only once rather than 3 times. To correct for this flaw, one solution is to calculate the contribution of these integration planes to the cone beam image filtered with the combined operation BD_rP, multiply this portion by a factor of 2, and add the result to the filtered cone beam image. The procedure is as follows. Construct the two common tangents at angles $\tau(\infty)$ and $\tau(-\infty)$ respectively connecting the top and bottom mask boundary curves diagonally. Then apply the combined operation BD_rP to the cone beam image in the limited angular range $\theta \in \mathscr{A}_2 = [\tau(-\infty)-\pi/2, \tau(\infty)+\pi/2]$, and only to those projections which do not intersect either the top or the bottom mask boundary. Applying Equations (2) and (4) yields the result that the procedure can be simplified as follows: for each angle $\alpha \in \mathscr{A}_2$, 1D Hilbert transform along the 2 lines in the direction of the unit vector $\vec{\alpha}$ which makes an angle α with the detector u axis and are tangential to the top and the bottom mask boundaries respectively. This procedure is illustrated in Figure 5.

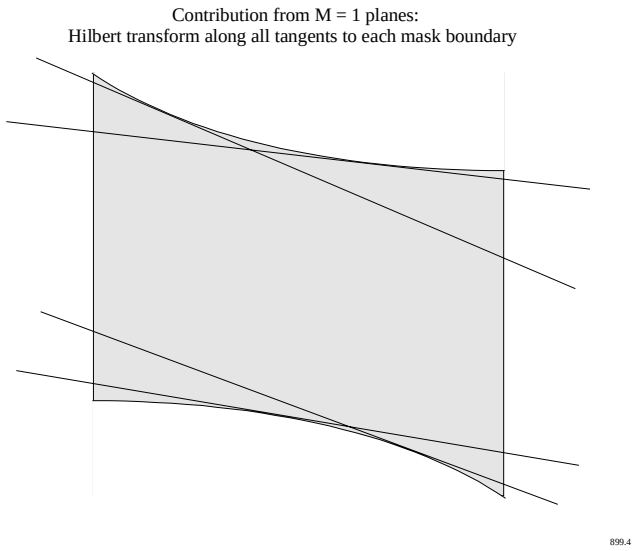

Figure 5. 1D Hilbert transforms illustrated at 2 of the angles $\in \mathcal{A}_2$.

V. Reduction of spiral overscan in long object solution

The results in Equations (2) and (4) are also applied to reduce the amount of overscan in the backprojection local ROI algorithm [3,4]. Briefly, the Hilbert transforms shown in Figure 2 can be used to determine which portion of the ROI is affected by the cone beam data at each source position near the spiral ends; those data that do not affect the ROI will not be needed. The details will be presented in [7].

VI. Acknowledgments

This work was supported in part by Bavarian Center of Excellence for Medical Imaging (FORBILD).

VII . References

1. Defrise, M. and Clack, R., "A Cone-Beam Reconstruction Algorithm Using Shift-Variant Filtering and Cone-Beam Backprojection", IEEE Trans.Med. Imag., MI-13, 186, 1994.
2. H. Kudo and T. Saito, “Derivation and Implementation of a Cone-Beam Reconstruction Algorithm for Nonplanar Orbits”, *IEEE Trans.Med. Imag*., MI-13, pp. 196-211, 1994.
3. K.C. Tam, “Exact local regions-of-interest reconstruction in spiral cone-beam filtered-backprojection CT: theory”, *Proc. of SPIE Medical Imaging Conf.*, vol. 3979, pp. 506-519, 2000
4. G. Lauritsch, K. C. Tam, K. Sourbelle, and S. Schaller, “Exact Local Regions-of-Interest in Spiral Cone-Beam Filtered-Backprojection CT: numerical implementation and first image results,” *Proc. of SPIE Medical Imaging Conf.*, 3979, pp. 520-532, 2000.
5. K.C. Tam, “Helical and circle scan region of interest computerized tomography”, *US. Patent* 5,463,666, Oct 31, 1995.
6. K.C. Tam, G. Lauritsch, and K. Sourbelle, “Eliminating the Second-Intersection Contributions to Spiral Scan Cone Beam CT”, IEEE Nucl. Sci. Symp. and Med. Imag. Conf. Conference Record, October 15-20, 2000, Lyon, France.
7. K.C. Tam, G. Lauritsch, and K. Sourbelle, “Overscan reduction in spiral scan long object problem”, to be submitted to IEEE Nucl. Sci. Symp. and Med. Imag. Conf., November 4-10, 2001, San Diego.
8. H. Kudo, F. Noo, and M. Defrise, "Cone-beam filtered-backprojection algorithm for truncated helical data", *Phys. Med. Biol*., 43, pp. 2885-2909, 1998.
9. K.C. Tam, B. Ladendorf, F. Sauer, G. Lauritsch, and A. Steinmetz, “Backprojection spiral scan region-of-interest cone beam CT”, *Proc. SPIE Medical Imaging 1999: Physics of Medical Imaging*, pp. 433-441, 1999.
10. G. Lauritsch, K. C. Tam, and K. Sourbelle, “Solution to the Long Object Problem by Convolutions with Spatially Variant 1-D Hilbert Transforms in Spiral Cone-Beam Computed Tomography”, IEEE Nucl. Sci. Symp. and Med. Imag. Conf. Conference Record, October 15-20, 2000, Lyon, France.
11. K.C. Tam, “A Method To Increase The Photon Counts For Enhanced Signal-To-Noise In Cone Beam CT”, Siemens Corporate Research invention disclosure IPD 99E9131 US, July 22, 1999.